Cellular and Molecular Life Sciences (2025) 82:130
https://doi.org/10.1007/s00018-025-05646-4

ORIGINAL ARTICLE

Endophilin B1 is essential for maintaining cardiac function by regulating mitocytosis

Jingyu Deng[1] · Xiaoqian Chang[1] · Xiaomeng Zhang[1] · Congye Li[1] · Guigao Guo[1] · Haifeng Song[1] · Yangzhi Zheng[1] · Chenhao Zhang[1] · Bo Yang[1] · Chujie Zhang[1] · Pingping Xing[1] · Zheng Zhang[2] · Tao Yin[1] · Ling Tao[1] · Shan Wang[1]

Received: 7 January 2025 / Revised: 24 February 2025 / Accepted: 4 March 2025

Abstract

Endophilin B1 is a member of the Endophilin family and has been shown to be involved in apoptosis, mitochondrial morphological changes and autophagy. Although Endophilin B1 is highly expressed in the heart, its role in the maintenance of normal cardiac function and myocardial ischemia and reperfusion (I/R) injury remains unclear. Here, we found that Endophilin B1 deletion provoked spontaneous cardiac contractile dysfunction, cardiac hypertrophy and fibrosis at 16 weeks of age. Moreover, at 8 weeks of age, although spontaneous cardiac dysfunction in Endophilin B1 deletion mice had not developed, the deletion of Endophilin B1 exacerbated I/R-induced cardiac contractile dysfunction and cardiomyocyte death, whereas restoration of Endophilin B1 expression in the heart reduced I/R injury. Furthermore, we discovered that Endophilin B1 is indispensable for maintaining normal mitochondrial structure and function. In addition, we found that Endophilin B1 is localized in extracellular mitochondrion-containing vesicles and is required for mitocytosis, a process by which damaged mitochondria are disposed through extracellular vesicles. In conclusion, our study identified Endophilin B1 as an essential mitocytosis regulator for maintaining mitochondrial homeostasis and cardiac function. These findings suggest that Endophilin B1 is a novel therapeutic target for cardiac disorders such as I/R injury, myocardial infarction and heart failure.

Keywords Endophilin B1 · Cardiac function · Extracellular vesicle · Mitocytosis

Introduction

Cardiomyocytes death occurs during myocardial ischemia-reperfusion (I/R) injury, which is related to reactive oxygen species (ROS) release, calcium overload, energy depletion, mitochondrial dysfunction, and apoptotic process activation [1]. Mitochondria have been recognized as a key trigger of cardiac I/R injury. Maintaining a well-functioning mitochondrial population is critical for cardiac homeostasis because damaged mitochondria produce less ATP and more ROS. The build-up of ROS destroys the complex of mitochondrial DNA, membrane phospholipids, and electron transport chain, leading to oxidative damage and ultimately cell death [2–5]. However, the regulatory mechanisms and biochemical contributions of mitochondrial dysfunction in cardiac I/R injury remain incompletely understood.

The Endophilin family is a group of proteins containing a carboxy-terminal SH3 (Src homology 3) structural domain and an amino-terminal BAR (Bin-amphiphysin-Rvs) structural domain [6, 7]. The SH3 domain plays a key role in forming complexes with proteins containing a proline-rich region (PRR), whereas the BAR domain is involved in protein–protein dimerization, membrane binding, and curvature formation and sensing [8]. In mammals, the Endophilin family consists of two subfamilies, Endophilin A and

Jingyu Deng, Xiaoqian Chang and Xiaomeng Zhang contributed equally to this work.

✉ Tao Yin
yintao@fmmu.edu.cn

✉ Ling Tao
lingtao@fmmu.edu.cn

✉ Shan Wang
wangshan1984@fmmu.edu.cn

[1] Department of Cardiology, Xijing Hospital, Fourth Military Medical University, 169 Changle West Road, Xi'an 710032, China

[2] Department of Cardiology, Rocket Force Characteristic Medical Center, Beijing 100088, China

Published online: 26 March 2025

Endophilin B, comprising Endophilins A1–A3 and B1 and B2, respectively. Endophilin A regulates clathrin-dependent endocytosis, including clathrin-encapsulated vesicle outgrowth, division, and decapsulation, and is involved in dynamin 1-mediated plasma membrane fission [9–14]. While the role of the Endophilin A family is well characterized, the physiological functions of Endophilin B family are not fully understood.

Endophilin B1, also known as SH3 domain-containing GRB2-like protein B1 (SH3GLB1) or Bax-interacting Factor 1 (Bif 1), is an Endophilin B protein. Endophilin B1 is expressed in most tissues, with high expression in the heart and skeletal muscle [15]. Studies have reported that Endophilin B1 plays a key role in cancer [16, 17], Parkinson's disease [18], Alzheimer's disease [19] and cerebral ischemic injury [20]. A recent study demonstrated that SUMO2-mediated SUMOylation of Endophilin B1 promotes ionizing radiation-induced hypertrophic cardiomyopathy [21]. However, whether Endophilin B1 is involved in maintaining normal cardiac function and myocardial I/R injury remains unclear. Furthermore, the molecular mechanism responsible for Endophilin B1 related cardiac regulation requires further investigation.

Therefore, in the present study, we aimed to investigate the role of Endophilin B1 in maintaining physiological cardiac function and myocardial I/R injury and to elucidate the potential molecular mechanisms involved.

Materials and methods

Animals

The animal experiments were conducted in accordance with the Guide for the Care and Use of Laboratory Animals, eighth edition (2011). All of the animal experimental protocols were reviewed and approved by the Fourth Military Medical University Committee on Animal Care. Endophilin B1 knockout (KO) mice (C57BL/6J background) and their wild-type (WT) littermates were established by Shanghai Model Organisms Center, Inc. The mice were maintained under identical temperature (22 ± 0.5 °C) and humidity (60 ± 5%) conditions and under a 12-h light–dark cycle. For this study, the animals were randomly assigned, and the experimenters were blinded to the results of the histological and in vivo functional assessments.

Myocardial I/R model

The myocardial I/R model was established as previously described [22]. In brief, adult male C57BL/6J and Endophilin B1-KO mice were anaesthetized with 2% isoflurane throughout the procedure. A left thoracotomy was performed to exteriorize the heart, and a silk suture (6–0) slipknot was reversibly tied around the left anterior descending (LAD) coronary artery. After 40 min of ischemia, reperfusion was induced by releasing the slipknot. Sham mice underwent the same procedure except for ligation around the left descending coronary artery.

Echocardiography

Twenty-four hours after the sham or I/R operation, the mice were anaesthetized with 2% isoflurane. M-mode images of the mice were obtained via an echocardiography system (Vevo 2100, VisualSonics, Canada), as previously described [23]. The hearts were viewed along the long axis between the two papillary muscles. Each measurement was obtained in M-mode by averaging the results from three consecutive heartbeats. The left ventricular ejection fraction (LVEF), left ventricular brachyaxis shortening (LVFS), and left ventricular internal dimensions (LVID) at diastole and systole (LVIDd and LVIDs) were measured.

Evaluation of cardiac infarct size

Cardiac infarct size was measured by Evans blue/triphenyltetrazolium chloride (TTC) staining after 24 h in the sham or I/R operation group, as previously described [24]. The mice were anaesthetized with 2% isoflurane, and the LAD coronary artery was re-ligated with a suture at the original ligature site. 2% Evans blue dye (Sigma, Cat No: E2129, USA) in PBS was injected into the brachiocephalic artery to visualize nonischemic tissue (blue area) and ischemic tissue (area at risk, AAR), and the hearts were extracted and sliced into five 1.0-mm-thick sections. The sections were subsequently incubated with 2% TTC (Sigma, Cat No: T8877, USA) in PBS at 37 °C for 5 min to visualize the infarct size (IS, white area) and viable myocardial tissue (red area). The red plus white area indicates the AAR. ImageJ software was used to measure the AAR and infarct area in the third section, and the values obtained were averaged.

Terminal deoxynucleotide transferase dUTP Nick end labelling (TUNEL) staining

TUNEL staining was performed via a Roche In Situ Cell Death Detection Kit (Roche, Cat No: 11684795910, Germany) following the manufacturer's instructions. The apoptosis index was determined by the number of TUNEL-positive nuclei/the total number of nuclei.

Concentrations of serum cardiac damage markers

To determine the concentrations of serum LDH, troponin T and CK-MB, blood was drawn from the carotid artery after 24 h of reperfusion. The serum was collected after centrifugation at 1000 rpm for 10 min at 4 °C and stored at -80 °C. The concentrations of LDH, troponin T and CK-MB were measured via an LDH ELISA kit (LSBio, Cat No: F54173, USA), a troponin T ELISA kit (ABclonal, Cat No: RK03251, China) and a CK-MB ELISA kit (LSBio, Cat No: F20753, USA), respectively, according to the manufacturers' instructions.

Masson's trichrome and wheat germ agglutinin staining

Heart tissues from Endophilin B1 KO and control mice were collected, fixed in 10% neutralized formalin, embedded in paraffin and sectioned into 5-μm-thick slices. The sections were stained with Masson's trichrome or wheat germ agglutinin (WGA) according to the manufacturer's protocol. The levels of collagen deposition were determined by Masson trichrome staining. After dyeing the cell nucleus for 5 min by wiegert's iron haematoxylin solution (Sigma-Aldrich, St. Louis, MO, USA), the sections were rinsed with distilled water 3 times, then stained with 0.7% Masson-Ponceau-acid fuchsin staining solution (Sigma-Aldrich) for 10 min. Following rinsing in 2% glacial acetic acid, samples were differentiated in phosphomolybdic acid for 4 min. Then 2% aniline blue dye solution (Sigma-Aldrich) was used to stain the sections. Following 100% ethanol for 5 min, Xylene for 5 min and sealing with neutral gum finally. And images were obtained with a microscope (Olympus SLIDEVIEW VS200, Japan). The collagen fibers (infarct area) were stained blue and normal myocardium were stained red.The degree of fibrosis was calculated as the ratio of the fibrotic area to the left ventricle area. For WGA staining, the cross-sectional area of cardiomyocytes was measured in images captured in sections stained with 5 μM WGA (Thermo, MA, United States) anda microscope (Olympus SLIDEVIEW VS200, Japan).

Adenovirus construction and administration

Adenoviruses carrying a specific plasmid for overexpressing Endophilin B1 (NM_ 019464.3) or adenoviruses carrying a negative control plasmid were designed and synthesized by *WZ Bioscience Inc*. (Shandong, China). The adenoviruses were delivered into the heart via intramyocardial injection as previously described [25]. In brief, the mice were anaesthetized with 2% isoflurane during the surgical procedure. After a left thoracic incision was made to expose the heart, the adenoviruses were resuspended in PBS at 1.5×10^{12} pfu/mL and intramyocardially injected at 3 different sites (10 μL per site) from the apex of the left ventricle free wall to the aortic root via a 30-gauge needle. Finally, the chest was carefully closed. On day 7 after adenovirus injection, the transduction efficiency of the adenovirus was examined via analysis of protein expression and the presence of GFP in the heart. Then, the mice underwent myocardial sham or I/R operation.

Cardiomyocyte isolation, culture, transfection and adenoviral infection

Neonatal mouse cardiomyocytes (NCMs) were isolated from 1- to 3-day-old neonatal C57BL/6J mice [22]. Briefly, the hearts of suckling mice were excised and fully washed with PBS under aseptic conditions. The ventricular tissues were minced with sterile scissors and digested with buffer containing 1 mg/mL collagenase type II (Gibco, Cat No: 17101015, USA) for 3 min at 37 °C. The digestion was repeated until the digestion mixture became clear (approximately 4–6 times). Cardiomyocytes were collected via differential plating and cultured in Dulbecco's modified Eagle's medium (DMEM) supplemented with 20% foetal bovine serum (FBS) and 1% penicillin–streptomycin. After another 48 h to allow the cardiomyocytes to completely plate, the NCMs were subjected to various treatments.

NCMs were transfected with the siRNA according to the manufacturer's protocol (Invitrogen™ Lipofectamine™ RNAiMAX, 13778075) for 6 h and then cultured in fresh complete medium for another 48 h before subsequent experiments. The sequences of the siRNAs targeting Endophilin B1 were as follows: sense, 5′-GCACAGUGUUACCAGUAUA; antisense, 5′-UAUACUGGUAACACUGUGC.

For adenoviral infection, NCMs were infected with recombinant adenoviruses for 6 h at an MOI of 50. The medium containing the virus was then replaced with fresh medium, and the cells were cultured for another 48 h. The efficiency of gene overexpression was detected by Western blot analysis.

Hypoxia/reoxygenation (H/R) model

Briefly, NCMs were cultured for 4 h in serum-free and glucose-free medium in a hypoxic chamber with 95% N_2 and 5% CO_2 at 37 °C. The NCMs were subsequently cultured in complete medium in an incubator supplemented with 21% O_2 and 5% CO_2 for 2 h to achieve reoxygenation.

Quantitative real-time PCR

Total RNA was extracted via TRIzol reagent (Thermo Fisher Scientific, Cat No: 15596026, USA). cDNA was synthesized via a PrimeScript™ RT Reagent Kit with gDNA Eraser (Takara, Cat No: RR047A, Japan), and quantitative RT–PCR was performed with SYBR® Premix Ex Taq™ II (Takara, Cat No: RR820L, Japan). Gene expression was calculated via the standard comparative CT method and normalized to the expression of GAPDH. The sequences of primers used were as follows: Endophilin B1: 5′-GTGTG AGCGGAGAGGCG-3′, 5′-TCTTCTGTGAACTGCACG GC-3′; GAPDH: 5′-GGAGCGAGATCCCTCC AAAAT-3′, 5′-GGCTGTTGTCATACTTCTCATGG-3′.

Western blot analysis

Heart tissues and NCMs were collected and lysed in RIPA lysis buffer. The proteins were electrophoresed and transferred to polyvinylidene difluoride (PVDF) membranes. Then, the membranes were blocked with 5% nonfat milk for 1 h and incubated with primary antibodies overnight at 4 °C. The primary antibodies used were as follows: HSP90 (1:1000, Cat No: 13171-1-AP, Proteintech, China), Endophilin B1 (1:1000, Cat No: sc-374146, Santa Cruz, USA), and cleaved caspase 3 (1:1000, Cat No: A11021, ABclonal, China). The membranes were incubated with secondary antibodies (1:5000, Cat No: 7074 S/7076S, CST, USA). The bands were visualized with enhanced chemiluminescence (ECL)-HRP (Cat No: WBAVDCH01, Millipore, USA) and analysed with Image Lab software (Bio-Rad, USA).

Seahorse analysis

The mitochondrial OCR was recorded with an XF24 Extracellular Flux Analyzer (Agilent Seahorse Bioscience, USA). Briefly, cardiomyocytes were seeded into XF24 Seahorse plates at a density of 160,000 cells/well and transfected with siRNA for 48 h. After the cells were subjected to normoxia or H/R, the OCR was measured according to the manufacturer's protocol. The optimal concentrations of the inhibitors were as follows: oligomycin, 0.6 μM; trifluoromethoxy carbonyl cyanide phenylhydrazone (FCCP), 0.75 μM; antimycin A, 2 μM; and rotenone, 1 μM. Basal respiration, maximal respiration, ATP production and spare respiration capacity were calculated via XF Cell Mito Stress Test Generator software (Agilent Seahorse Bioscience, USA). Basal respiration and maximal respiration were obtained using the XF Cell Mito Stress Test Generator software (Agilent Seahorse Bioscience). ATP production and spare respiration capacity were obtained by calculation.

Transmission electron microscopy

Heart pieces and NCMs were first fixed with 4% glutaraldehyde in PBS overnight at 4 °C. The samples were subsequently fixed in 1% osmium tetroxide for 1 h. Then, the rings were dehydrated, embedded in resin and cut into 80-nm-thick sections. The samples were examined via transmission electron microscopy (JEM-1230, JEOL Ltd., Japan) at 80 kV. Mitochondrial size was analysed via ImageJ software.

Detection of mitochondrial reactive oxygen species (ROS)

Mitochondrial ROS were detected with the fluorescent probe MitoSOX (Invitrogen, Cat No: M36008, USA) following the manufacturer's protocols. Images were obtained with a confocal laser scanning microscope (FV3000, Olympus, Japan) and analysed with ImageJ software.

Mitochondrial membrane potential measurements

The mitochondrial membrane potential (Δψm) was measured with JC-1 kits (Beyotime, China) according to the manufacturer's instructions. NCMs were incubated in JC-1 staining solution at 37 °C for 20 min. Cells with a normal mitochondrial membrane potential presented red fluorescence (570 nm), while JC-1 release emitted green fluorescence (535 nm) in damaged cells with mitochondrial membrane potential depolarization. The ratio of red (aggregate JC-1)/green (monomeric JC-1) fluorescence intensity was detected via a confocal microscope (FV3000, Olympus, Japan) and was proportional to the Δψm.

Statistical analysis

The data are expressed as the means ± standard deviations. An unpaired Student's *t* test was performed for analysis of differences between two groups. One-way or two-way ANOVA followed by Tukey's post hoc test or post hoc paired/unpaired t tests with Bonferroni correction was used for multiple group comparisons. All the statistical analyses were performed with GraphPad Prism 6.0 (GraphPad Software, La Jolla, CA, USA). $P < 0.05$ indicated statistical significance.

Results

Endophilin B1 deficiency provokes spontaneous cardiac contractile dysfunction, cardiac hypertrophy and fibrosis

We first examined the expression profiles of Endophilin B1 in different tissues/organs, including the heart, brain, liver, skeletal muscle, kidney, lung, spleen and white adipose tissues, and detected the highest protein and mRNA levels of Endophilin B1 in the heart (Fig. S1A–C). To assess the effects of Endophilin B1 on cardiac physiology and disease, we generated Endophilin B1 KO mice (Fig. S2A). Western blot analysis confirmed the absence of Endophilin B1 protein in the hearts of Endophilin B1 KO mice (Fig. S2B and C). The contents of fasting serum glucose, triglyceride and total cholesterol were not significantly different between Endophilin B1 KO mice and control WT mice at 8, 16 and 24 weeks of age (Fig. S2D–F). Echocardiography analysis was used to detect cardiac contractile function in Endophilin-B1 KO and control WT mice at 8, 16 and 24 weeks of age. No significant cardiac dysfunction was observed at 8 weeks of age. However, by 16 weeks of age, we observed a significant decrease in cardiac contractile function, which was exemplified by a decreased LVEF, decreased LVFS, and increased LVIDs and LVIDd (Fig. 1A–E), in Endophilin B1 KO mice compared with control WT mice. Moreover, at 24 weeks of age, we observed a progressive decline in cardiac contractile function in Endophilin-B1 KO mice (Fig. 1A–E). Furthermore, Endophilin B1 KO mice presented a greater cross-sectional area of myocytes and more myocardial interstitial fibrosis at 16 weeks of age (Fig. 1F–I). Additionally, Endophilin B1 KO mice presented significantly reduced viability at 15 weeks of age (Fig. 1J). These data showed that Endophilin B1 deficiency results in spontaneous cardiac contractile dysfunction, cardiac hypertrophy and fibrosis without pathological stress.

Endophilin B1 deficiency exacerbates I/R-induced cardiac contractile dysfunction and cardiomyocyte death

We next determined Endophilin B1 expression after cardiac I/R injury. Western blot analysis revealed that the protein levels of Endophilin B1 were significantly lower in the heart tissues of I/R model mice than in those of sham model mice (Fig. 2A). Consistent with these results, qPCR assays showed that the mRNA levels of Endophilin B1 were significantly reduced in the heart after I/R injury (Fig. 2B). We also subjected mouse neonatal cardiomyocytes (NCMs) to hypoxia for 4 h and reoxygenation for 2 h (H/R) and revealed decreased protein and mRNA levels of Endophilin B1 in H/R-treated NCMs (Fig. S3A–C). These results indicated a strong association between decreased Endophilin B1 expression and cardiac I/R injury.

To gain insight into the function of reduced Endophilin B1 in cardiac I/R injury, we subjected Endophilin B1 KO and control WT mice to I/R surgery or a sham operation at 8 weeks of age, a time point at which spontaneous cardiac dysfunction has not developed in Endophilin B1 KO mice. Echocardiography was used to evaluate cardiac function at 1 day post-I/R. Both Endophilin B1 KO and control WT mice subjected to I/R presented significantly decreased cardiac contractile function compared with their respective sham mice (Fig. 2C–G). Notably, Endophilin-B1 deficiency significantly aggravated I/R-induced cardiac contractile dysfunction (Fig. 2C–G). We next measured cardiac infarct size via Evans blue and TTC double staining and found that Endophilin B1 deficiency markedly increased the I/R-induced myocardial infarct size (Fig. 2H–J). In agreement with these results, Endophilin B1 deficiency increased the I/R-induced elevations in the serum concentrations of LDH, CK-MB and troponin T (Fig. 2K–M). Furthermore, Endophilin B1 deficiency increased the number of TUNEL-positive cells in the left ventricular ischemic area, which indicated increased apoptosis (Fig. 2N and O).

To determine whether Endophilin B1 defect directly caused cardiomyocyte apoptosis, we isolated NCMs and then infected them with siRNA targeting Endophilin B1 or a control scrambled siRNA. Western blot and qPCR analyses revealed that the siRNA effectively knocked down Endophilin B1 expression (Fig. S4A–C). As expected, TUNEL staining analysis demonstrated that Endophilin B1 knockdown in NCMs significantly promoted cell apoptosis under H/R conditions compared with that in the control group (Fig. S4D and E). Additionally, Endophilin B1 knockdown in NCMs significantly increased the H/R-induced expression of cleaved caspase 3 (Fig. S4F and G).

Taken together, our data indicate that Endophilin B1 defects are critical for I/R-induced cardiac contractile dysfunction and cardiomyocyte death.

Adenoviral intramyocardial endophilin B1 transfer improves I/R-induced cardiac contractile dysfunction and cardiomyocyte death

To determine whether Endophilin B1 overexpression can rescue I/R-induced cardiac dysfunction, we restored Endophilin B1 expression by injecting adenoviruses expressing the Endophilin B1-GFP fusion protein into mouse hearts. Seven days after injection, these mice were subjected to I/R surgery or a sham operation (Fig. S5A). We observed GFP-positive cardiomyocytes scattered around the injection site in the left ventricular myocardium at 7

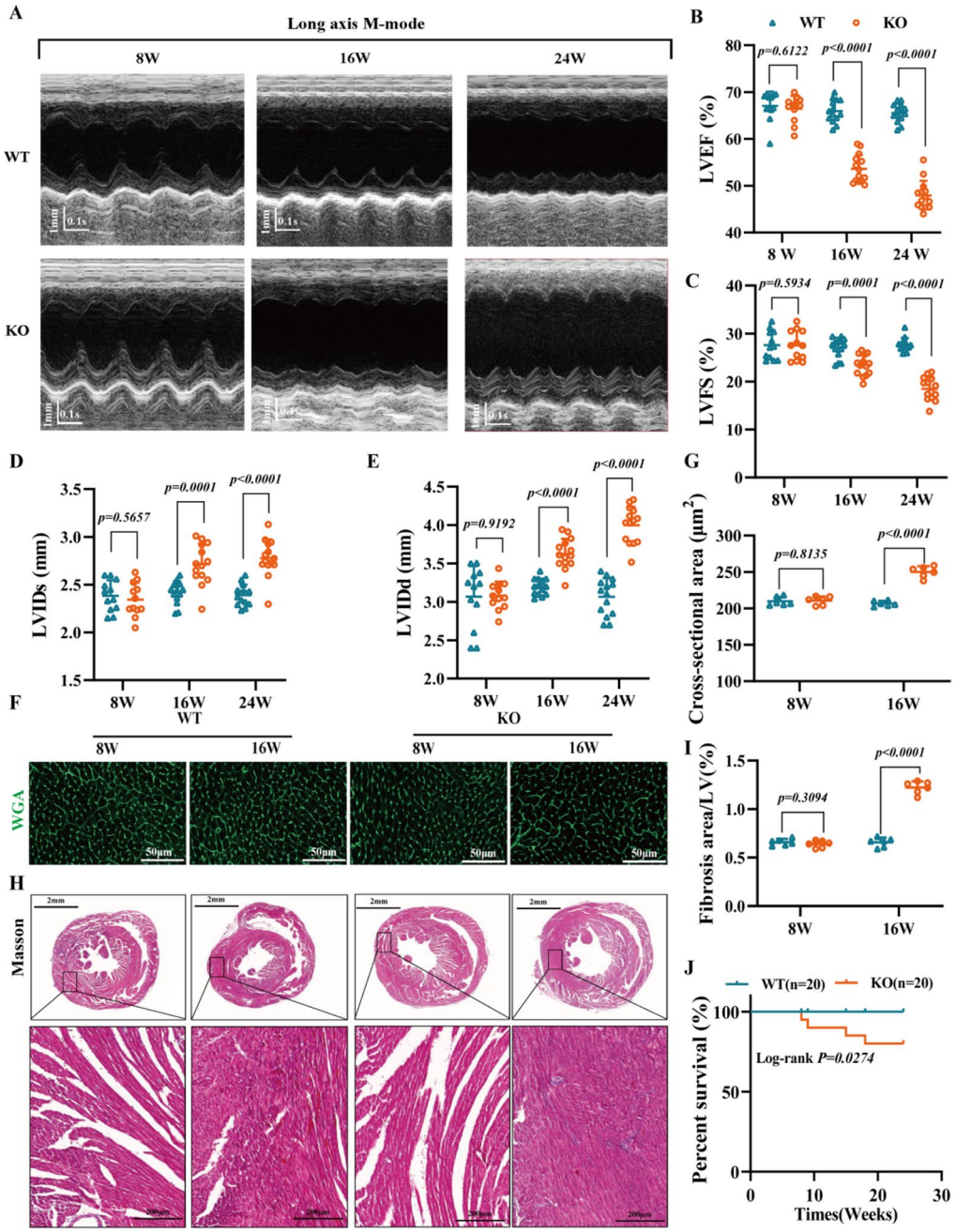

Fig. 1 Endophilin B1 deficiency results in contractile dysfunction, cardiac hypertrophy and fibrosis. **A** Representative long-axis M-mode echocardiographic images from male control (WT) and Endophilin B1 KO (KO) mice. **B–E** Left ventricular ejection fraction (LVEF, **B**), left ventricular shortening fraction (LVFS, **C**), left ventricular diastolic internal dimension (LVIDd, **D**) and left ventricular systolic internal dimension (LVIDs, **E**) were measured via long-axis M-mode echocardiography ($n=12/14$). **F** and **G** Representative microscopy image of immunohistochemical staining for WGA and quantification of its cross-sectional area. Scale bars: 50 μm. $n=6$/group. **H** and **I** Representative images of heart sections stained with Masson's trichrome and quantification of the fibrotic areas. Scale bars: 2 mm (top) and 200 μm (bottom). $n=6$/group. **J** Postnatal survival curves of male controls ($n=20$) and Endophilin B1 KO mice ($n=20$). The data are presented as the means ± SDs. The data in J were analysed via log-rank Mantel–Cox tests. Other data were analysed via two-way ANOVA, followed by Tukey's post hoc test. 8 W, 8 weeks; 16 W, 16 weeks; 24 W, 24 weeks

days post-injection (Fig. S5B). Significant overexpression of Endophilin B1 was observed in the hearts of the mice injected with Ad-Endophilin B1 (Fig. S5C and D). The echocardiography results revealed that Endophilin B1 overexpression alleviated I/R-induced cardiac contractile dysfunction (Fig. 3A–E) and reduced the I/R-induced myocardial infarct size (Fig. 3F–H). Furthermore, Endophilin B1 overexpression in the heart resulted in resistance to

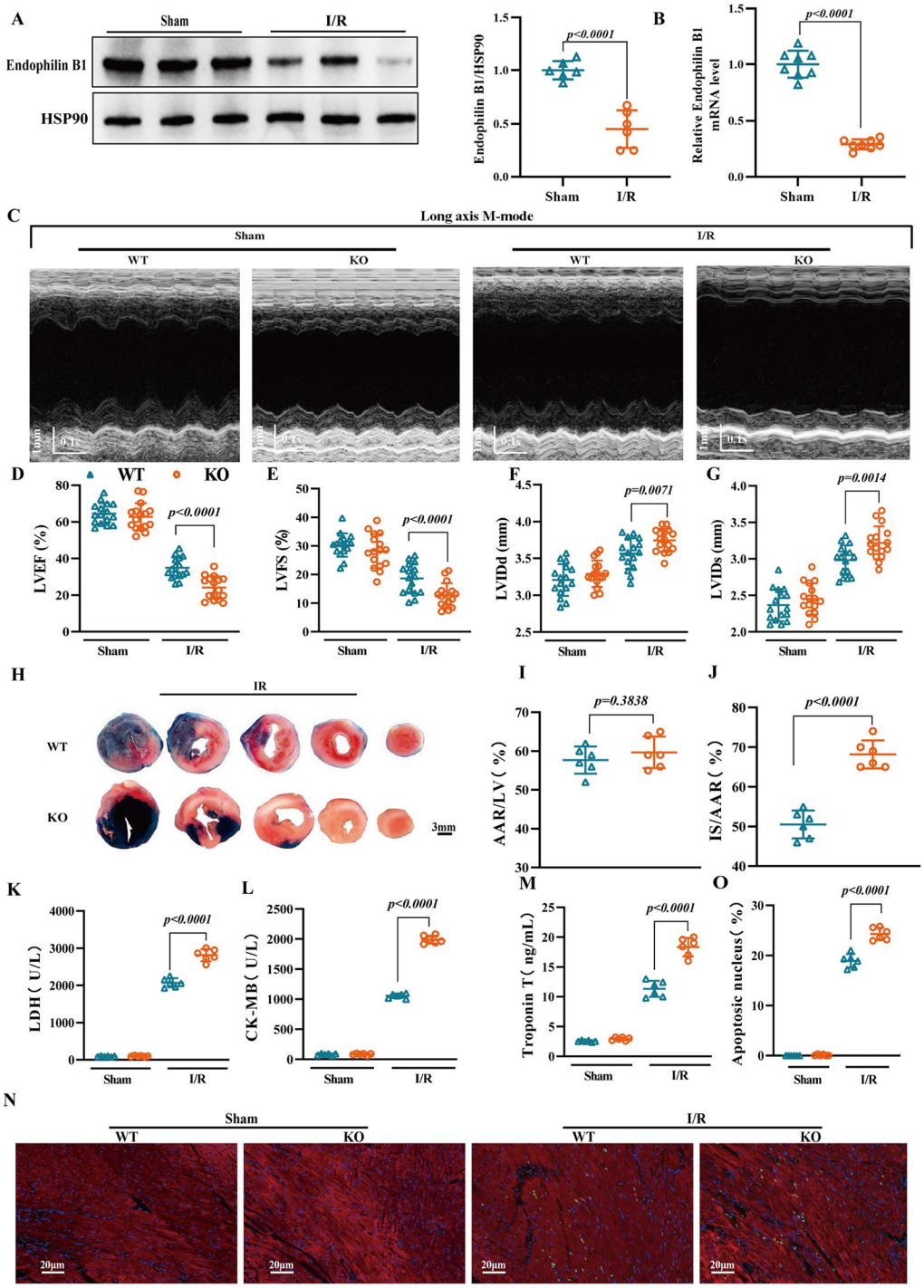

Fig. 2 Endophilin B1 deficiency exacerbates I/R injury. **A** Representative Western blot and quantification of Endophilin B1 protein levels in sham hearts or the infarct border zone of male mouse heart tissues after 40 min of ischemia followed by 24 h of reperfusion. $n=6$/group. **B** Relative Endophilin B1 mRNA levels in sham hearts or the infarct border zone of male mouse heart tissues after 35 min of ischemia followed by 24 h of reperfusion. $n=8$/group. **C** Representative long-axis M-mode echocardiographic images from mice 1 day after sham or I/R surgery. **D–G** LVEF (**D**), LVFS (**E**), LVIDd (**F**) and LVIDs (**G**) were measured by long-axis M-mode echocardiography. $n=16$/group. **H–J** Representative images of Evans blue and TTC staining and assessment of the area at risk (AAR)/left ventricle (LV) and infarct size (IS)/AAR for hearts from mice 1 day after I/R surgery. The blue area represents unaffected heart tissue; the white area represents infarcted tissue; and the red plus white area represents the tissue at risk. Scale bar: 3 mm. $n=6$/group. **K–M** The concentrations of serum cardiac damage markers, including lactate dehydrogenase (LDH, **K**), creatine kinase-MB (CK-MB, **L**) and troponin T (**M**), were determined via ELISA kits. $n=6$/group. **N–O** Representative images and quantitative analysis of TUNEL-stained heart sections. Scale bar: 20 μm. $n=6$/group. The data are expressed as the means ± SDs. The data in A and B were analysed via unpaired, 2-tailed Student's t test. Other data were analysed via two-way ANOVA, followed by Tukey's post hoc test

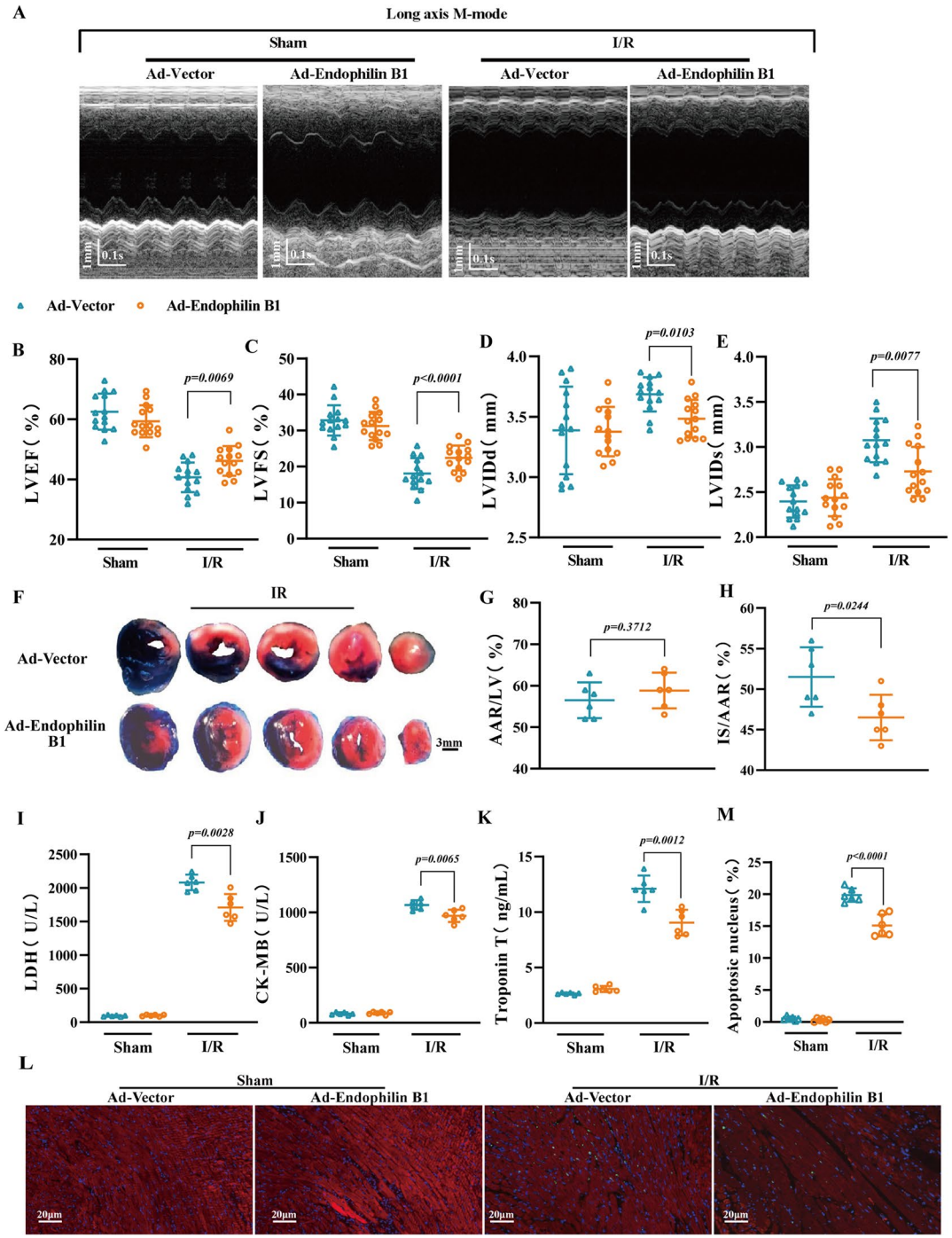

Fig. 3 Endophilin B1 overexpression in the heart alleviates I/R injury. **A** Representative long-axis M-mode echocardiographic images from mice 1 day after sham or I/R surgery. **B–E** LVEF (**B**), LVFS (**C**), LVIDd (**D**) and LVIDs (**E**) were measured by long-axis M-mode echocardiography. $n=14$/group. **F–H** Representative images of Evans blue and TTC staining and assessment of the AAR/LV and IS/AAR for hearts from mice 1 day after I/R surgery. Scale bar: 3 mm. $n=6$/group. **I–K** The concentrations of serum cardiac damage markers, including LDH (**I**), CK-MB (**J**) and troponin T (**K**), were determined via ELISA kits. $n=6$/group. **L–M**: Representative images and quantitative analysis of TUNEL-stained heart sections. Scale bar: 20 μm. $n=6$/group. The data are presented as the means ± SDs. The data were analysed via two-way ANOVA, followed by Tukey's post hoc test

I/R-induced necrosis, as indicated by reductions in LDH levels and CK-MB and troponin T release (Fig. 3I–K). In addition, Endophilin B1 overexpression decreased the number of TUNEL-positive cells in the left ventricular ischemic area, which suggested decreased apoptosis (Fig. 3L and M).

To demonstrate whether restoring Endophilin B1 directly decreases H/R-induced cardiomyocyte apoptosis, we overexpressed Endophilin B1 in NCMs via adenovirus infection. Western blot and qPCR analyses revealed that the adenoviral vector carrying Endophilin B1 significantly increased the expression of Endophilin B1 in NCMs. (Fig. S6A–C). As expected, compared with NCMs infected with adenoviral empty vectors, Endophilin B1 overexpression significantly reduced cell apoptosis under H/R conditions (Fig. S6D and E). Additionally, Endophilin B1 overexpression in NCMs significantly decreased the H/R-induced expression of cleaved caspase 3 (Fig. S6F and G).

Overall, our data revealed that restoring Endophilin B1 expression in the heart improved I/R-induced cardiac contractile dysfunction and cardiomyocyte death.

Endophilin B1 deficiency results in mitochondrial morphological abnormalities

Cardiomyocyte survival and function are closely correlated with mitochondrial homeostasis. We next examined myocardial mitochondrial morphology via transmission electron microscopy (TEM) in Endophilin B1 KO and control WT mice at 8 and 16 weeks of age, respectively. No significant alterations in mitochondrial morphology were observed in Endophilin B1 KO mice compared with control WT mice at 8 weeks of age. However, at 16 weeks of age, we found that Endophilin B1 KO provoked mitochondrial morphological abnormalities, as indicated by greater swelling, a decreased number of mitochondrial cristae, a reduced cristae area (Fig. 4A–D), and a significantly reduced number of mitochondria per μm^2 (Fig. 4E). These findings indicate that defects in Endophilin B1 impair mitochondrial structure in the heart.

Endophilin B1 knockdown in NCMs aggravates H/R-induced mitochondrial damage

Given that Endophilin B1 deficiency impairs myocardial mitochondrial structure, we next determined whether Endophilin B1 can directly affect mitochondrial function in cardiomyocytes. Therefore, we used confocal microscopy images and quantitative analysis of mitochondrial ROS production to assess mitochondrial ROS levels and found that Endophilin B1 knockdown increased mitochondrial ROS production in NCMs under H/R conditions (Fig. 5A and B). We also tested the mitochondrial membrane potential via JC-1 staining and found that Endophilin B1 knockdown significantly decreased the mitochondrial membrane potential in NCMs under H/R conditions (Fig. 5C and D). Given these profound changes in mitochondrial structure and mitochondrial oxidative damage, we analysed the mitochondrial OCR to assess the mitochondrial respiratory capacity. As expected, Endophilin B1 knockdown significantly suppressed mitochondrial respiratory capacity, as indicated by basal respiration, ATP production, maximal respiration and spare respiration, in NCMs under HR conditions (Fig. 5E and F). Taken together, these data demonstrate that Endophilin B1 knockdown exacerbates H/R-induced mitochondrial membrane potential loss and increases mitochondrial ROS production and mitochondrial respiratory dysfunction.

Endophilin B1 overexpression in NCMs ameliorates H/R-induced mitochondrial damage

To further demonstrate the role of Endophilin B1 in H/R-induced mitochondrial injury, we overexpressed Endophilin B1 in NCMs through adenovirus infection. As expected, Endophilin B1 overexpression significantly reduced mitochondrial ROS production after H/R compared with that in NCMs infected with adenoviral empty vectors (Fig. 6A and B). Moreover, JC-1 staining revealed that Endophilin B1 overexpression attenuated the H/R-induced loss of the mitochondrial membrane potential in NCMs (Fig. 6C and D). We further analysed the mitochondrial OCR to assess the mitochondrial respiratory capacity and found that Endophilin B1 overexpression significantly improved the mitochondrial respiratory capacity, as indicated by basal respiration, ATP production, maximal respiration and spare respiration, in NCMs under HR conditions (Fig. 6E and F). Collectively, our data demonstrate that Endophilin B1 overexpression in NCMs alleviates H/R-induced mitochondrial membrane potential loss and increases mitochondrial ROS production and respiratory dysfunction.

Endophilin B1 is localized in extracellular mitochondrion-containing vesicles and promotes mitocytosis

To understand how Endophilin B1 regulates mitochondrial function, we infected NCMs with adenoviruses expressing the Endophilin B1-GFP fusion protein and then treated them with MitoTracker (red) to observe whether Endophilin B1 and mitochondria were colocalized. Interestingly, we found that Endophilin B1 localized to extracellular vesicles, many of which contain mitochondria, in NCMs under HR conditions (Fig. 7A). Cardiomyocytes eject dysfunctional mitochondria in extracellular vesicles to control mitochondrial quality and thus support cardiomyocyte function [25]. This

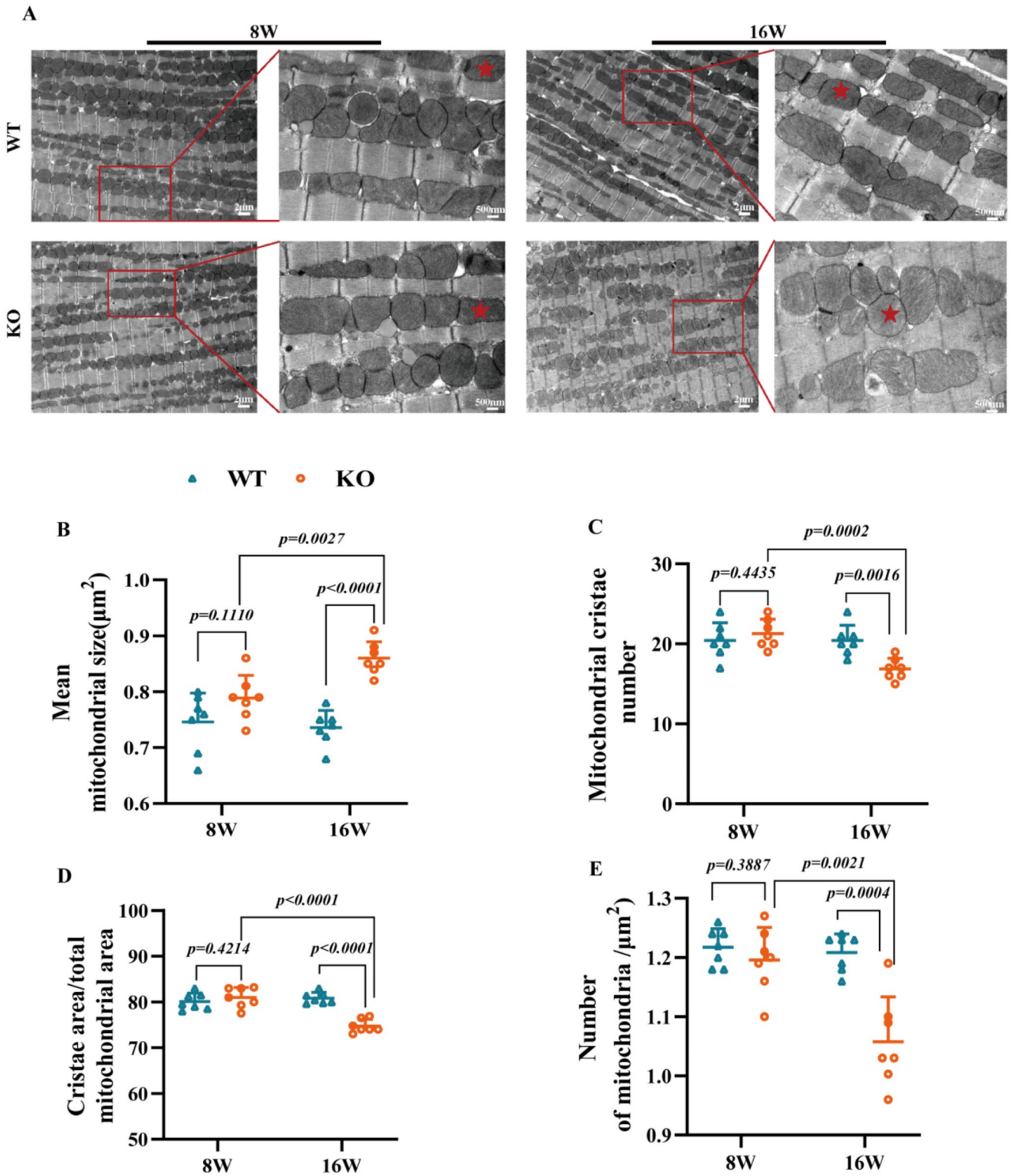

Fig. 4 Endophilin B1 deficiency provokes mitochondrial morphological abnormalities. **A** Representative TEM images of myocardial mitochondria (magnification ×6000 [6 K] and ×20,000 [20 K]) and quantitative analysis of mitochondrial size (**B**), cristae number (**C**), cristae area (**D**) and number of mitochondria per μm^2 (**E**). Scale bar at 6 K: 2 μm; scale bar at 20 K: 500 nm. $n=7$/group. The data are presented as the means ± SDs. The data were analysed via two-way ANOVA, followed by Tukey's post hoc test

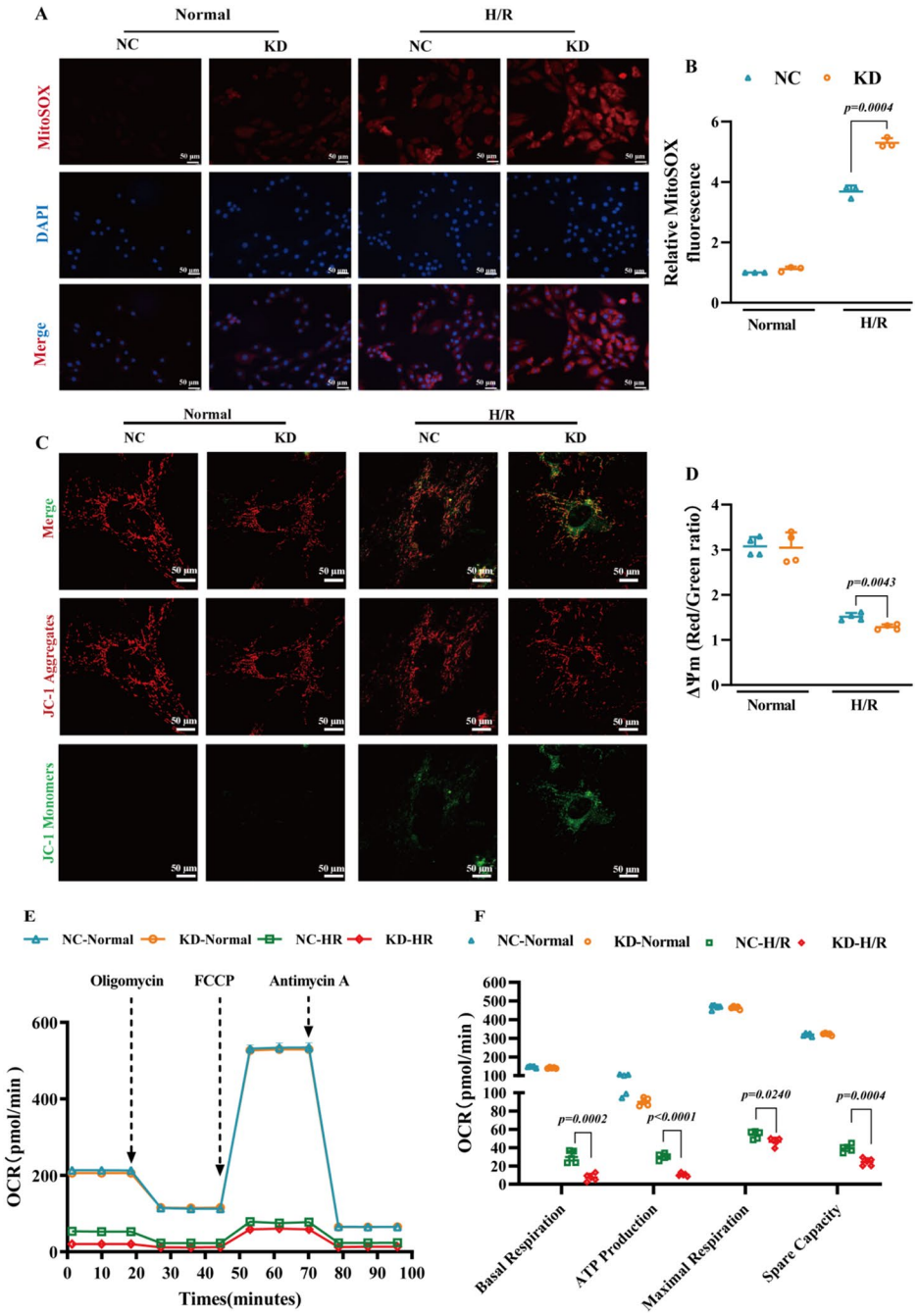

Fig. 5 Endophilin B1 knockdown in NCMs aggravated H/R-induced mitochondrial injury. **A–B** Representative confocal microscopy images and quantitative analysis of mitochondrial ROS production (MitoSOX fluorescence; red) in control (NC) or Endophilin B1-knockdown (KD) NCMs under normal or H/R conditions. Scale bar: 50 μm. $n=3$/group. **C–D** Immunofluorescence analysis and quantification of the mitochondrial membrane potential by JC-1 staining in control (NC) or Endophilin B1-knockdown (KD) NCMs under normal or H/R conditions. Scale bar: 50 μm, $n=4$/group. **E–F** Measure of the OCR and respective quantitative analysis of mitochondrial respiratory capacity, including basal respiration, ATP production, maximal respiration and spare respiration, in control (NC) or Endophilin B1-knockdown (KD) NCMs under normal or H/R conditions. $n=5$/group. The data are presented as the means ± SDs. The data were analysed via two-way ANOVA, followed by Tukey's post hoc test. FCCP, trifluoromethoxy carbonyl cyanide phenylhydrazone

process of disposing damaged mitochondria via extracellular vesicles has also been found in neutrophils and is named mitocytosis [26]. We next examined whether Endophilin B1 is involved in mitocytosis. We stained NCMs with WGA (red) and MitoTracker (green) and found that Endophilin B1 knockdown blocked mitochondrion-containing vesicle secretion in NCMs under HR conditions (Fig. 7B). TEM images of NCMs also demonstrated that Endophilin B1 knockdown markedly inhibited the secretion of mitochondrion-containing vesicles under HR conditions (Fig. 7C). The majority of mitochondria inside these vesicles exhibited morphological abnormalities. In addition, TEM of heart sections revealed that compared with control WT mice, Endophilin B1 KO mice presented reduced extracellular mitochondrion-containing vesicle secretion and more severe mitochondrial damage such as greater swelling, a decreased number of mitochondrial cristae, a reduced cristae area at 1 day post-I/R (Fig. 7D-G). In parallel, Endophilin B1 overexpression in the heart increased extracellular mitochondrion-containing vesicle secretion and ameliorated I/R-induced mitochondrial morphological abnormalities (Fig. 7D-G). Taken together, these data suggest that

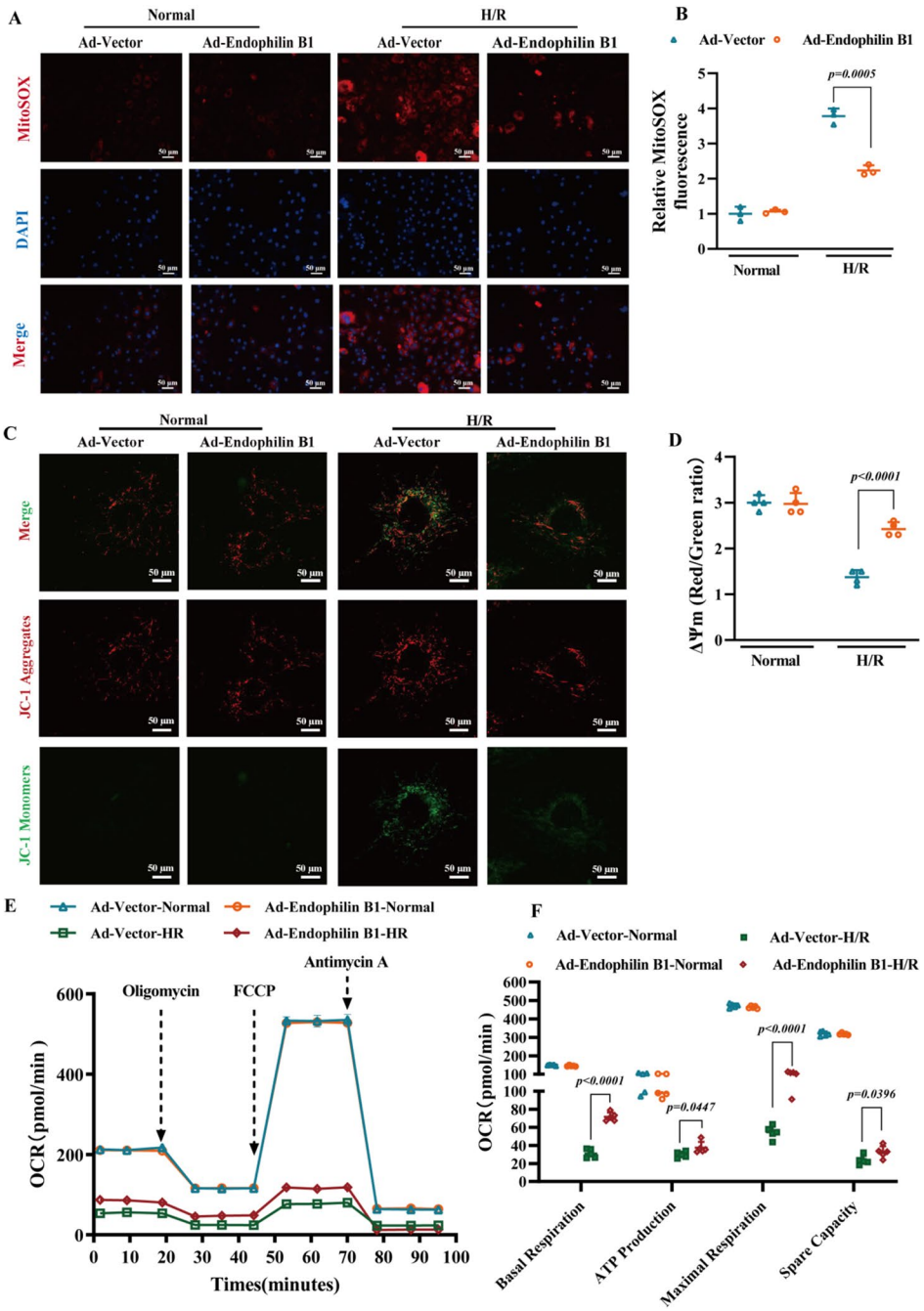

Fig. 6 Endophilin B1 overexpression in NCMs protects against H/R-induced mitochondrial injury. **A–B** Representative confocal microscopy images and quantitative analysis of mitochondrial ROS production (MitoSOX fluorescence; red) in control (Ad-Vector) or Endophilin B1-overexpressing (Ad-Endophilin B1) NCMs under normal or H/R conditions. Scale bar: 50 μm. $n=3$/group. **C–D** Immunofluorescence analysis and quantification of the mitochondrial membrane potential by JC-1 staining in control (Ad-Vector) or Endophilin B1-overexpressing (Ad-Endophilin B1) NCMs under normal or H/R conditions. Scale bar: 50 μm, $n=4$/group. **E–F** Measure of the OCR and respective quantitative analysis of mitochondrial respiratory capacity, including basal respiration, ATP production, maximal respiration and spare respiration, in control (Ad-Vector) or Endophilin B1-overexpressing (Ad-Endophilin B1) NCMs under normal or H/R conditions. $n=5$/group. The data are presented as the means ± SDs. The data were analysed via two-way ANOVA, followed by Tukey's post hoc test

Endophilin B1 is localized in extracellular mitochondrion-containing vesicles and is required for mitocytosis.

Discussion

The myocardium is the most energy-consuming tissue in the human body; thus, it uniquely relies on a large number of functional mitochondria to continuously produce high-energy phosphates. It is therefore not surprising that mitochondria are critical targets and the root of myocardial I/R injury, which is at the centre of the pathology of the most common cardiovascular diseases [27]. Endophilin B1 has been shown to be highly expressed in the heart [15]. Moreover, Endophilin B1 defect altered the morphology of mitochondria in both HeLa cells and neurons [20, 28]. However, the roles of Endophilin B1 in maintaining normal cardiac function and myocardial I/R injury remain unclear. Here, we found that Endophilin B1 deletion resulted in spontaneous development of cardiac contractile dysfunction, cardiac hypertrophy and fibrosis. Both gain- and loss-of-function experiments highlighted the requisite role of Endophilin

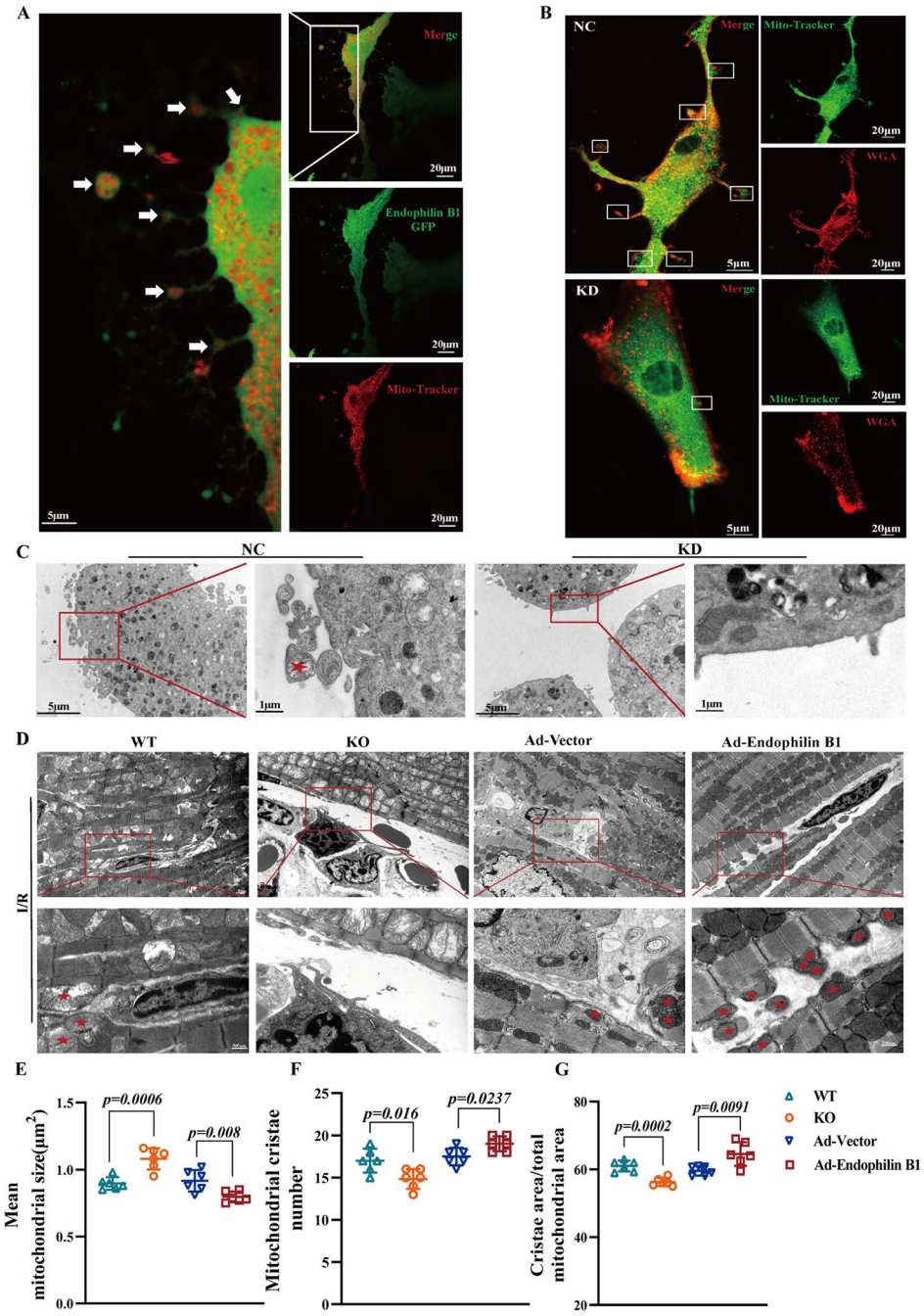

Fig. 7 Endophilin-B1 is localized in extracellular mitochondrion-containing vesicles and promotes the secretion of damaged mitochondria. **A** Representative confocal image of Endophilin B1-GFP-expressing NCMs under H/R conditions stained with MitoTracker (red). Scale bar: 5 μm (left); 20 μm (right). **B** Representative confocal images of control (NC) or Endophilin B1-knockdown (KD) NCMs under H/R conditions stained with MitoTracker (green) and WGA (red). Scale bar: 5 μm (left); 20 μm (right). **C** Representative TEM images of control (NC) or Endophilin B1-knockdown (KD) NCMs under H/R conditions. Scale bar: 5 μm (left); 1 μm (right). **D** Representative TEM images of myocardial mitochondria and quantitative analysis of mitochondrial size (**E**), cristae number (**F**), cristae area (**G**). Scale bar: 2 μm (top); 500 nm (bottom); $n = 6$/group. The data are expressed as the means ± SDs. The data in E, F and G were analysed via unpaired, 2-tailed Student's t test

B1 in protecting the heart against I/R injury in vivo. Moreover, we elucidated the indispensable role of Endophilin B1 in preserving mitochondrial homeostasis through promoting mitocytosis. Our findings reveal a novel link between Endophilin B1 and mitochondrial quality control and identify Endophilin B1 as a potential therapeutic target to counteract ischemic heart disease.

Several novel findings were uncovered in the present study. First, we suggest that Endophilin B1 plays an essential role in maintaining cardiac contractile function under physiological conditions. The Endophilin family consists of five isoforms, Endophilins A1–A3, B1 and B2, which are distributed in various tissues [29]. Northern blot analysis revealed that Endophilin B1 is expressed in most tissues and is highly expressed in the heart and skeletal muscle [15]. However, whether Endophilin B1 is involved in maintaining normal cardiac function remains unknown. In this study, among tissues/organs, including heart, brain, liver, skeletal muscle, kidney, lung, spleen and white adipose tissues, we found that endophilin B1 was most highly expressed in the heart. Using a systemic Endophilin B1 deletion mouse model, we found that Endophilin B1 deletion did not significantly affect

cardiac function in 8-week-old mice. However, Endophilin B1 deletion caused the mice to develop progressive cardiac contractile dysfunction, cardiac hypertrophy and fibrosis at 16 weeks. These findings demonstrate a physiological role for Endophilin B1 in maintaining normal cardiac function.

Second, we demonstrated that downregulation of Endophilin B1 contributes to myocardial I/R injury. We found that the protein and mRNA levels of Endophilin B1 were reduced in mouse hearts after I/R injury and in NCMs under H/R conditions. Endophilin B1 deletion exacerbated I/R-induced cardiac contractile dysfunction and cardiomyocyte death. In parallel, the restoration of Endophilin B1 expression in the heart protects the heart from I/R injury. These findings suggest that Endophilin B1 is a promising therapeutic target for counteracting cardiac I/R injury. Endophilin B1 was initially identified as a proapoptotic protein and acted as a novel Bax binding partner and activator in FL5.12 murine pre-B haematopoietic cells [15]. Loss of Endophilin B1 in either HeLa cells or mouse embryonic fibroblasts suppresses the Bax/Bak conformational change and mitochondrial apoptosis induced by various intrinsic death signals [17]. In contrast, Endophilin B1 has been reported to function as a prosurvival factor in neurons. Endophilin B1 knockdown exacerbates apoptosis induced by the DNA-damaging agent camptothecin in mouse primary cortical neurons [20]. Endophilin B1 overexpression promotes oxygen and glucose deprivation followed by reperfusion-induced cortical neuron survival and reduces the cell apoptotic rate [30]. In addition, Endophilin B1-deficient mice developed larger infarcts after middle cerebral artery occlusion, suggesting that Endophilin B1 deficiency exacerbates ischemic injury-induced neuron death [20]. However, another study demonstrated that Endophilin B1 knockdown attenuated 1-methyl-4-phenylpyridinium (MPP+) and mutant α-synuclein-mediated cell death in cultured cortical neurons [18]. The reason for the opposite effects of endophilin B1 on cell death and survival may be that the levels or activity of Endophilin B1 can either decrease or increase depending on the type of injury; normalization of Endophilin B1 function in either direction may have a protective effect.

Third, we identified Endophilin B1 as an essential regulator for preserving mitochondrial homeostasis in cardiomyocytes. Endophilin B1 knockdown altered the distribution and morphology of mitochondria and resulted in the dissociation of the outer mitochondrial membrane and intermitochondrial membrane compartments in HeLa cells [28]. Moreover, neurons from Endophilin B1-deficient mice contained fragmented mitochondria, and Endophilin B1 knockdown in wild-type neurons also resulted in fragmented mitochondria, which were more depolarized [6]. Here, we found that Endophilin B1 deficiency reduced the number of mitochondria and provoked mitochondrial morphological abnormalities in the myocardium. Moreover, Endophilin B1 knockdown aggravated, whereas Endophilin B1 overexpression ameliorated, H/R-induced mitochondrial dysfunction in NCMs. This evidence suggests that Endophilin B1 is indispensable for preserving mitochondrial morphology and function and thus supports normal cardiac function.

Finally, we report for the first time that Endophilin B1 is localized in extracellular mitochondrion-containing vesicles and is required for mitocytosis. Recently, cardiomyocytes were shown to eject dysfunctional mitochondria and other material in subcellular vesicles, which were named exophers, into the extracellular space. The extruded material is readily taken up and processed by a network of resident macrophages that surround cardiomyocytes, thus supporting heart homeostasis [25]. Jiao et al. reported that, upon exposure to mild mitochondrial stresses, damaged mitochondria are transported into migrasomes and subsequently disposed from migrating cells. They named this process mitocytosis [26]. However, the molecular mechanism regulating mitocytosis is unclear. In this study, we found that Endophilin B1 is localized in extracellular mitochondrion-containing vesicles. Endophilin B1 defects reduce mitocytosis in cardiomyocytes and aggravate I/R-induced mitochondrial morphological abnormalities. While, Endophilin B1 overexpression in the heart increased mitocytosis and ameliorated I/R-induced mitochondrial damage. These data suggest that Endophilin B1 is required for cardiomyocyte mitocytosis. Previous studies have demonstrated that Endophilin B1 is involved in autophagosome biogenesis [21,, 25, 31]. The formation of exophers containing dysfunctional mitochondria and other material ejected from cardiomyocytes is driven by the autophagy machinery [32]. Another study established that lysosomal inhibition leads to increased secretion of mitochondria in large extracellular vesicles, which are produced in multivesicular bodies, and that the release of large extracellular vesicles is independent of autophagy [33]. Further studies are needed to determine whether Endophilin B1 promotes mitocytosis by regulating autophagy.

There are some limitations of our study. Firstly, further studies are needed to determine whether Endophilin B1 promotes mitocytosis by regulating autophagy. Secondly, we fail to establish the cardiac-specifc Endophilin B1 KO mice to explore the effect of Endophilin B1 on myocardial I/R injury in current study. Thirdly, even though we identified Endophilin B1 is required for the secretion of damaged mitochondrion-containing vesicles, we cannot exclude other possible mechanisms that contribute to protect against myocardial I/R injury. Finally, although many conclusions have been drawn on the basis of mouse models in vivo and in vitro, further preclinical and clinical studies are needed to

confirm these results. Despite these limitations, we believe that our findings provide important novel insights for understanding the protective roles of Endophilin B1 and the underlying regulatory mechanisms in myocardial I/R injury.

Conclusion

In conclusion, our study identified Endophilin B1 as a critical regulator for preserving cardiac function and attenuating cardiac I/R injury. Endophilin B1 is required for the secretion of damaged mitochondrion-containing vesicles, thus supporting mitochondrial homeostasis. These data suggest that Endophilin B1 is a novel therapeutic target for cardiac disorders such as I/R injury, myocardial infarction and heart failure.

Supplementary Information The online version contains supplementary material available at https://doi.org/10.1007/s00018-025-05646-4.

Acknowledgements We thank all members of the L. Tao's lab for useful suggestions.

Author contributions SW, LT, TY, JYD, XQC and XMZ conceived and designed the research; JYD, XQC, XMZ, CYL, GGG, HFS, YZZ, CHZ, BY, CJZ and PPX, ZZ performed the experiments, analysed the data, interpreted the results of the experiments and prepared the figures; SW, LT, TY, JYD, XQC and XMZ drafted the manuscript; all the authors contributed to editing, revision, and approved the final version of the manuscript.

Funding This work was financially supported by the Program for National Science Funds of China (Grant Nos. 82070867, 82330009, 81970721 and 81927805), the Program for Changjiang Scholars and Innovative Research Team in University (Grant No. PCSIRT-14R08), and the Xijing Hospital Innovative Medical Research Project (XJZT-24CY48).

Data Availability The datasets used and/or analysed during the current study are available from the corresponding author on reasonable request.

Declarations

Ethical approval All animal experiments were carried out according to the National Institutes of Health Guidelines on the Use of Laboratory Animals (NIH Publication, 8th Edition, 2011) and were approved by the Fourth Military Medical University Committee on Animal Care.

Conflict of interest The authors declare no competing interests.

References

1. Heusch G (2020) Myocardial ischaemia-reperfusion injury and cardioprotection in perspective. Nat Rev Cardiol 17(12):773–789. https://doi.org/10.1038/s41569-020-0403-y
2. Kuznetsov AV, Javadov S, Margreiter R, Grimm M, Hagenbuchner J, Ausserlechner MJ (2019) The role of mitochondria in the mechanisms of cardiac Ischemia-Reperfusion injury. Antioxid (Basel Switzerland) 8(10):454. https://doi.org/10.3390/antiox8100454
3. Wang J, Zhou H (2020) Mitochondrial quality control mechanisms as molecular targets in cardiac ischemia-reperfusion injury. Acta Pharm Sinica B 10(10):1866–1879. https://doi.org/10.1016/j.apsb.2020.03.004
4. Chen CL, Zhang L, Jin Z, Kasumov T, Chen YR (2022) Mitochondrial redox regulation and myocardial ischemia-reperfusion injury. Am J Physiol Cell Physiol 322(1):C12–C23. https://doi.org/10.1152/ajpcell.00131.2021
5. Cai W, Liu L, Shi X, Liu Y, Wang J, Fang X, Chen Z, Ai D, Zhu Y, Zhang X (2023) Alox15/15-HpETE aggravates myocardial Ischemia-Reperfusion injury by promoting cardiomyocyte ferroptosis. Circulation 147(19):1444–1460. https://doi.org/10.1161/CIRCULATIONAHA.122.060257
6. Sparks AB, Hoffman NG, McConnell SJ, Fowlkes DM, Kay BK (1996) Cloning of ligand targets: systematic isolation of SH3 domain-containing proteins. Nat Biotechnol 14(6):741–744. https://doi.org/10.1038/nbt0696-741
7. Gallop JL, Jao CC, Kent HM, Butler PJ, Evans PR, Langen R, McMahon HT (2006) Mechanism of endophilin N-BAR domain-mediated membrane curvature. EMBO J 25(12):2898–2910. https://doi.org/10.1038/sj.emboj.7601174
8. Li J, Barylko B, Eichorst JP, Mueller JD, Albanesi JP, Chen Y (2016) Association of endophilin B1 with cytoplasmic vesicles. Biophys J 111(3):565–576. https://doi.org/10.1016/j.bpj.2016.06.017
9. Gad H, Ringstad N, Löw P, Kjaerulff O, Gustafsson J, Wenk M, Di Paolo G, Nemoto Y, Crun J, Ellisman MH, De Camilli P, Shupliakov O, Brodin L (2000) Fission and uncoating of synaptic clathrin-coated vesicles are perturbed by disruption of interactions with the SH3 domain of endophilin. Neuron 27(2):301–312. https://doi.org/10.1016/s0896-6273(00)00038-6
10. Pechstein A, Gerth F, Milosevic I, Jäpel M, Eichhorn-Grünig M, Vorontsova O, Bacetic J, Maritzen T, Shupliakov O, Freund C, Haucke V (2015) Vesicle uncoating regulated by SH3-SH3 domain-mediated complex formation between endophilin and intersectin at synapses. EMBO Rep 16(2):232–239. https://doi.org/10.15252/embr.201439260
11. Ringstad N, Gad H, Löw P, Di Paolo G, Brodin L, Shupliakov O, De Camilli P (1999) Endophilin/SH3p4 is required for the transition from early to late stages in clathrin-mediated synaptic vesicle endocytosis. Neuron 24(1):143–154. https://doi.org/10.1016/s0896-6273(00)80828-4
12. Sundborger A, Soderblom C, Vorontsova O, Evergren E, Hinshaw JE, Shupliakov O (2011) An endophilin-dynamin complex promotes budding of clathrin-coated vesicles during synaptic

vesicle recycling. J Cell Sci 124(Pt 1):133–143. https://doi.org/10.1242/jcs.072686
13. Verstreken P, Kjaerulff O, Lloyd TE, Atkinson R, Zhou Y, Meinertzhagen IA, Bellen HJ (2002) Endophilin mutations block clathrin-mediated endocytosis but not neurotransmitter release. Cell 109(1):101–112. https://doi.org/10.1016/s0092-8674(02)00688-8
14. Watanabe S, Mamer LE, Raychaudhuri S, Luvsanjav D, Eisen J, Trimbuch T, Söhl-Kielczynski B, Fenske P, Milosevic I, Rosenmund C, Jorgensen EM (2018) Synaptojanin and endophilin mediate neck formation during ultrafast endocytosis. Neuron 98(6):1184–1197e6. https://doi.org/10.1016/j.neuron.2018.06.005
15. Cuddeback SM, Yamaguchi H, Komatsu K, Miyashita T, Yamada M, Wu C, Singh S, Wang HG (2001) Molecular cloning and characterization of Bif-1. A novel Src homology 3 domain-containing protein that associates with Bax. J Biol Chem 276(23):20559–20565. https://doi.org/10.1074/jbc.M101527200
16. Takahashi Y, Hori T, Cooper TK, Liao J, Desai N, Serfass JM, Young MM, Park S, Izu Y, Wang HG (2013) Bif-1 haploinsufficiency promotes chromosomal instability and accelerates Myc-driven lymphomagenesis via suppression of mitophagy. Blood 121(9):1622–1632. https://doi.org/10.1182/blood-2012-10-459826
17. Takahashi Y, Karbowski M, Yamaguchi H, Kazi A, Wu J, Sebti SM, Youle RJ, Wang HG (2005) Loss of Bif-1 suppresses Bax/Bak conformational change and mitochondrial apoptosis. Mol Cell Biol 25(21):9369–9382. https://doi.org/10.1128/MCB.25.21.9369-9382.2005
18. Wong AS, Lee RH, Cheung AY, Yeung PK, Chung SK, Cheung ZH, Ip NY (2011) Cdk5-mediated phosphorylation of endophilin B1 is required for induced autophagy in models of Parkinson's disease. Nat Cell Biol 13(5):568–579. https://doi.org/10.1038/ncb2217
19. Wang DB, Kinoshita Y, Kinoshita C, Uo T, Sopher BL, Cudaback E, Keene CD, Bilousova T, Gylys K, Case A, Jayadev S, Wang HG, Garden GA, Morrison RS (2015) Loss of endophilin-B1 exacerbates Alzheimer's disease pathology. Brain 138(Pt 7):2005–2019. https://doi.org/10.1093/brain/awv128
20. Wang DB, Uo T, Kinoshita C, Sopher BL, Lee RJ, Murphy SP, Kinoshita Y, Garden GA, Wang HG, Morrison RS (2014) Bax interacting factor-1 promotes survival and mitochondrial elongation in neurons. J Neuroscience: Official J Soc Neurosci 34(7):2674–2683. https://doi.org/10.1523/JNEUROSCI.4074-13.2014
21. Gao A, Zou J, Mao Z, Zhou H, Zeng G (2022) SUMO2-mediated sumoylation of SH3GLB1 promotes ionizing radiation-induced hypertrophic cardiomyopathy through mitophagy activation. Eur J Pharmacol 924:174980. https://doi.org/10.1016/j.ejphar.2022.174980
22. Gao E, Lei YH, Shang X, Huang ZM, Zuo L, Boucher M, Fan Q, Chuprun JK, Ma XL, Koch WJ (2010) A novel and efficient model of coronary artery ligation and myocardial infarction in the mouse. Circul Res 107(12):1445–1453. https://doi.org/10.1161/CIRCRESAHA.110.223925
23. Xia Y, Zhang F, Zhao S, Li Y, Chen X, Gao E, Xu X, Xiong Z, Zhang X, Zhang J, Zhao H, Wang W, Wang H, Guo Y, Liu Y, Li C, Wang S, Zhang L, Yan W, Tao L (2018) Adiponectin determines farnesoid X receptor agonism-mediated cardioprotection against post-infarction remodelling and dysfunction. Cardiovascular Res 114(10):1335–1349. https://doi.org/10.1093/cvr/cvy093
24. Gao C, Wang R, Li B, Guo Y, Yin T, Xia Y, Zhang F, Lian K, Liu Y, Wang H, Zhang L, Gao E, Yan W, Tao L (2020) TXNIP/Redd1 signalling and excessive autophagy: a novel mechanism of myocardial ischaemia/reperfusion injury in mice. Cardiovascular Res 116(3):645–657. https://doi.org/10.1093/cvr/cvz152
25. Nicolás-Ávila JA, Lechuga-Vieco AV, Esteban-Martínez L, Sánchez-Díaz M, Díaz-García E, Santiago DJ, Rubio-Ponce A, Li JL, Balachander A, Quintana JA, Martínez-de-Mena R, Castejón-Vega B, Pun-García A, Través PG, Bonzón-Kulichenko E, García-Marqués F, Cussó L, A-González N, González-Guerra A, Roche-Molina M, Hidalgo A (2020) Heart Cell 183(1):94–109e23. A Network of Macrophages Supports Mitochondrial Homeostasis https://doi.org/10.1016/j.cell.2020.08.031
26. Jiao H, Jiang D, Hu X, Du W, Ji L, Yang Y, Li X, Sho T, Wang X, Li Y, Wu YT, Wei YH, Hu X, Yu L (2021) Mitocytosis, a migrasome-mediated mitochondrial quality-control process. Cell 184(11):2896–2910e13. https://doi.org/10.1016/j.cell.2021.04.027
27. Niemann B, Schwarzer M, Rohrbach S (2018) Heart and mitochondria: pathophysiology and implications for cardiac surgeons. Thorac Cardiovasc Surg 66(1):11–19. https://doi.org/10.1055/s-0037-1615263
28. Karbowski M, Jeong SY, Youle RJ (2004) Endophilin B1 is required for the maintenance of mitochondrial morphology. J Cell Biol 166(7):1027–1039. https://doi.org/10.1083/jcb.200407046
29. Yang LQ, Huang AF, Xu WD (2023) Biology of endophilin and it's role in disease. Front Immunol 14:1297506. https://doi.org/10.3389/fimmu.2023.1297506
30. Yun Q, Jiang M, Wang J, Cao X, Liu X, Li S, Li B (2015) Overexpression Bax interacting factor-1 protects cortical neurons against cerebral ischemia-reperfusion injury through regulation of ERK1/2 pathway. J Neurol Sci 357(1–2):183–191. https://doi.org/10.1016/j.jns.2015.07.027
31. Takahashi Y, Coppola D, Matsushita N, Cualing HD, Sun M, Sato Y, Liang C, Jung JU, Cheng JQ, Mulé JJ, Pledger WJ, Wang HG (2007) Bif-1 interacts with Beclin 1 through UVRAG and regulates autophagy and tumorigenesis. Nat Cell Biol 9(10):1142–1151. https://doi.org/10.1038/ncb1634
32. Takahashi Y, Meyerkord CL, Wang HG (2008) BARgaining membranes for autophagosome formation: regulation of autophagy and tumorigenesis by Bif-1/Endophilin B1. Autophagy 4(1):121–124. https://doi.org/10.4161/auto.5265
33. Liang W, Sagar S, Ravindran R, Najor RH, Quiles JM, Chi L, Diao RY, Woodall BP, Leon LJ, Zumaya E, Duran J, Cauvi DM, De Maio A, Adler ED, Gustafsson ÅB (2023) Mitochondria are secreted in extracellular vesicles when lysosomal function is impaired. Nat Commun 14(1):5031. https://doi.org/10.1038/s41467-023-40680-5